

Prediction of solid solubility in alloys

J. A. Alonso* and S. Simozar

*Department of Materials Science and Engineering, University of Pennsylvania, Philadelphia, Pennsylvania 19104
and Laboratory for Research on the Structure of Matter, University of Pennsylvania, Philadelphia, Pennsylvania 19104*

(Received 5 August 1980)

A new empirical method for the analysis of solid solubility in alloys is proposed. The method is an extension of previous work by Darken and Gurry and by Chelikowsky. Each chemical element is characterized by three parameters: the atomic volume V , the electronegativity ϕ^* , and the electron density at the boundary of bulk atomic cells n_b . $\Delta\phi^*$ and Δn_b (Δ indicates the difference between solvent and solute) are combined into a unique parameter, ΔH_c , the heat of formation of an equiatomic compound. This is done by using the semiempirical theory of Miedema and co-workers. Then, the two parameters ΔH_c and ΔV are used to construct a two-dimensional map. In this map, the chemical elements insoluble in a given host are neatly separated from the soluble ones. Even more, it seems that contours of increasing degree of solubility can be drawn with a fair degree of success.

I. INTRODUCTION: REVIEW OF THE PREDICTION OF SOLID SOLUBILITY IN ALLOYS

The prediction of solid solubility in alloys has attracted the interest of metallurgists and solid-state physicists since the early 1930's. The first significant contribution was made by Hume-Rothery,¹ who proposed three empirical rules (or factors) to explain the formation of solid solutions: (1) the atomic sizes of the solvent and solute must not differ by more than 15%, (2) the electrochemical nature of the two elements must be similar, and (3) a higher-valent metal is more soluble in a lower-valent metal than vice versa. Only the first rule is a quantitative rule, whereas the other two rules only have a qualitative character. Scientific basis for the two first rules was given by Friedel² and Eshelby.³ Darken and Gurry⁴ were able to make the second rule quantitative by bringing into play the concept of electronegativity, introduced by Pauling.⁵ Darken and Gurry introduced a map where the two coordinates are the electronegativity and the atomic size. Each chemical element is represented by a point on this map. Then they found that an ellipse which is centered on the solvent and has one axis of $\pm 15\%$ of the solvent's size and another axis of ± 0.4 of an electronegativity unit of the solvent's electronegativity value would encompass most of the solutes which show significant solubility in the solvent. An extensive analysis performed by Waber and co-workers⁶ showed that the Darken-Gurry method predicts extensive solid solutions with a 60% confidence level, limited solid solutions with an 82% confidence level, and an overall reliability of 80%. By comparison, the confidence levels of the simple size rule of Hume-Rothery are 50.1, 90.3, and

67.6%, respectively. The Darken-Gurry method has been used by several authors.⁷ Gschneidner⁷ has extended the Darken-Gurry method to slightly improve the reliability of the predictions. The main new feature in the set of rules formulated by Gschneidner has been the introduction of the crystal structure of the pure components as a new parameter and the selective use of the Hume-Rothery method for the cases where the crystal-structure factor is favorable.

A graphical procedure similar to the Darken-Gurry plots has recently been introduced by Chelikowsky.⁸ This author used, nevertheless, a different pair of coordinates: the electron density at the boundary of bulk atomic cells, n_b , and the electronegativity ϕ^* . These two coordinates are the fundamental parameters in a successful semiempirical theory of heats of alloy formation developed by Miedema and co-workers.⁹⁻¹¹ The relation of the Miedema coordinates to more fundamental descriptions of the alloy-formation problem has been attempted by several authors.¹²⁻¹⁸ In this new kind of plot, Chelikowsky was able to draw an ellipse containing most of the metals which are soluble in a given host metal. The position of the host metal lies inside the ellipse, although the precise location varies from host to host. Chelikowsky analyzed the solid solubility for the case of divalent hosts and he demonstrated that the use of the Miedema coordinates in the graphical method gives more accurate predictions than the use of the Darken-Gurry coordinates. A few cases are found which disagree with Chelikowsky's prediction. We mention, for instance, the case of silicon in beryllium. Si is predicted to be soluble, a fact which disagrees with the experimental in-

formation. Other examples are plutonium and scandium, as solutes in magnesium. Pu and Sc are both predicted to be insoluble in Mg, whereas the experimental result is the opposite. A few other exceptions are found in the figures published by Chelikowsky.⁸ These exceptions suggest that Chelikowsky's method is still susceptible to some improvement. An interesting point to note is that the Darken-Gurry plot, although less successful than Chelikowsky's plot, is still a good first approximation for the prediction of solid solubilities. Both graphical methods have a coordinate in common—the electronegativity (the fact that Pauling's scale⁵ is normally used in the Darken-Gurry plots, whereas the Miedema scale used in Chelikowsky's plot is of minor importance: both scales show a good correlation⁹). The second coordinate is different: atomic size in one case and electron cell-boundary density in the other case. It seems to us that a scheme containing all three coordinates should be more successful.¹⁹ We show in the next section how the three coordinates can be handled and combined in order to arrive at a two-dimensional graphical representation in the spirit of the work mentioned above. We first show that the predictions of solid solubility are improved. The relative importance of the three coordinates is clearly displayed. Finally, the considerable success of the schemes of Darken and Gurry and of Chelikowsky is explained by the fact that atomic size and electron cell-boundary density are strongly correlated, although the correlation is not complete. This accounts for the exceptions observed in the Darken-Gurry and Chelikowsky plots.

II. PARAMETRIC ANALYSIS OF SOLID SOLUBILITY

Figures 1 and 2 show a Chelikowsky plot for the solubility in iron and cobalt, respectively. The two coordinates characteristic of each metal, electronegativity (ϕ^*) and electron cell-boundary density (n_b), have been taken from the tabulation of Miedema *et al.*¹¹ The solutes have been divided into four classes: (a) solutes with a measured solubility higher than 15 at. %, (b) those for which the solubility is between 5 and 15 at. %, (c) those for which the solubility is between 1 and 5 at. %, and (d) solutes with a solubility smaller than 1 at. %. The solubility refers to the maximum solid solubility (at a temperature no higher than the melting temperature of the pure solute; we have found this restriction convenient to eliminate some exceptions). The experimental information on the solubility was taken from Refs. 20 and 21. Both figures show that an ellipse can be drawn which

contains most of the highly soluble elements and leaves the insoluble elements outside. Some exceptions are also noted. For instance, B, Ag, and U are insoluble in Fe. In contrast, these three elements are found inside or very near to the ellipse of high solubility. Ti is at a distance from the ellipse which is greater than the distance of Pu, U, Ta, or Nb, despite the fact that Ti is more soluble than Pu, U, Ta, or Nb. Some exceptions are also found in the graph for Co (Fig. 2). B, Ag, and U are again inside the ellipse of high solubility, despite the fact that these three elements are insoluble in Co. Two of the exceptions in Fig. 2, lithium and calcium, deserve a separate comment. The only data on the solubility of these two elements are very old²² and by the same author in both cases. These two elements deviate so strongly from the expected solubility behavior (see also Fig. 4) that we have strong doubts about the reliability of the experimental results. A new experimental determination of the solubility of Li and Ca in Co would be welcomed. The main observation from Figs 1 and

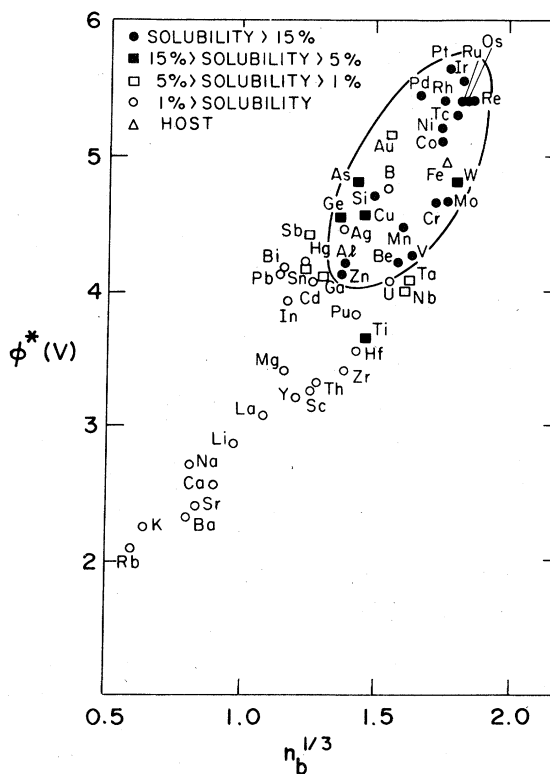


FIG. 1. Chelikowsky's plot for the analysis of solid solubility in Fe. The two coordinates of each element are the electronegativity ϕ^* and the electron-density parameter $n_b^{1/3}$ of the Miedema theory of heats of formation. An ellipse is drawn which separates soluble from insoluble elements.

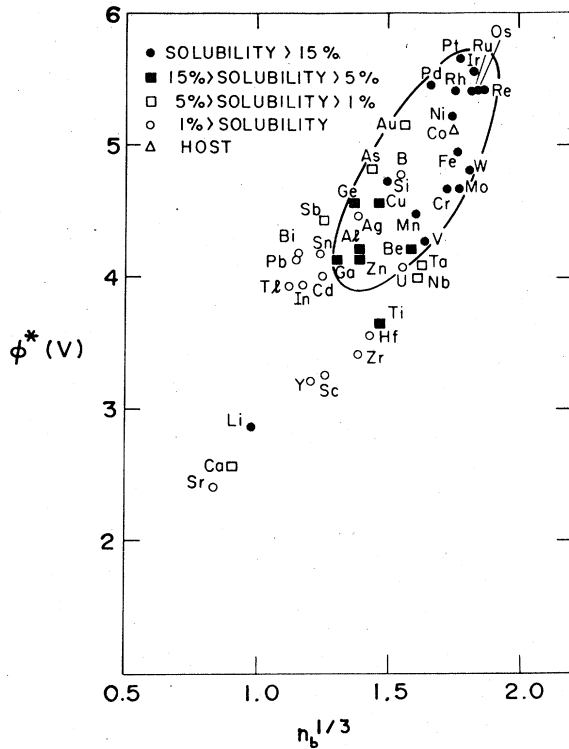


FIG. 2. Same as Fig. 1 although the host is Co.

2 is that there is no way to draw a sharp separation contour between the insoluble elements (for example, those with a solubility smaller than 1%) and the soluble ones. If one remembers that the Hume-Rothery size rule (as well as the Darken-Gurry method) is rather successful in predicting insolubility, we can try to improve the predictions of Figs. 1 and 2 by introducing a third coordinate, the atomic size. We characterize the atomic size by the radius R_{ws} of the Wigner-Seitz sphere of the metal (radius of a sphere with a volume equal to the volume per atom in the pure metal). We then have three coordinates— ϕ^* , n_b , and R_{ws} . In order to conserve the pictorial simplicity of a two-dimensional plot we have combined ϕ^* and n_b (more precisely, the differences $\Delta\phi^*$ and Δn_b between the two alloy partners) into a single coordinate, the heat of formation ΔH_c of a fictitious 50/50 intermetallic compound formed by the two partners. To calculate ΔH_c we use the semiempirical formula proposed by Miedema⁹⁻¹¹:

$$\Delta H_c = -P(\Delta\phi^*)^2 + Q(\Delta n_b^{1/3})^2 - R. \quad (1)$$

In this equation, P and Q are universal constants, whereas R is another constant which is different from zero only when one of the partners is a poly-

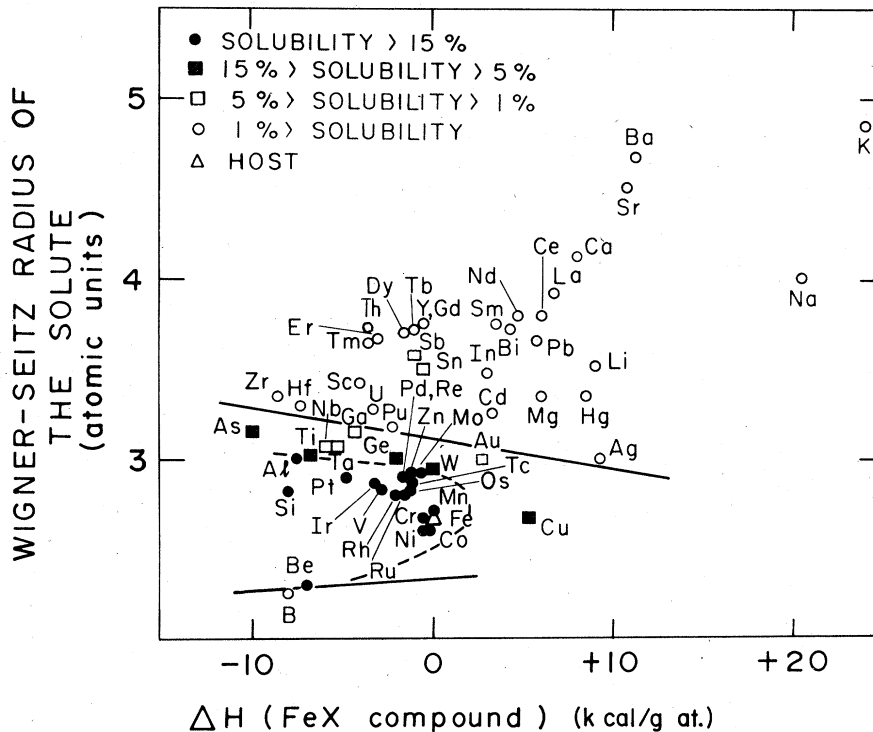


FIG. 3. Wigner-Seitz radius of the solute X versus the heat of formation of the compound FeX . The two continuous lines separate the insoluble elements from the rest. The broken line encloses the highly soluble (solubility larger than 15 at. %) elements.

valent metal with p electrons.⁹⁻¹¹ Then we plotted a two-dimensional map. Each alloy FeX (or CoX) is represented by a point on this map. The first coordinate of the point is ΔH_{FeX} (or ΔH_{CoX}), whereas the second coordinate is $R_{ws}(X)$, the Wigner-Seitz radius of the pure solute. In a few nonmetal cases (Si, Ge, As, Sb, Bi) the Wigner-Seitz radius is not the one corresponding to the stable pure-solute phase, but the radius of a more convenient metallic phase, as proposed by Miedema.¹¹ For some of the alloys treated here, ΔH_{FeX} (or ΔH_{CoX}) has been tabulated by Miedema.^{10,23} Figure 3 shows that it is possible to separate sharply the insoluble elements (solubility smaller than 1%) from the soluble ones. A continuous line has been drawn to show this. The only exceptions are Sn and Sb. The experimental data on these two alloys are very old. Furthermore, the solubility has not been measured at temperatures below the melting point of Sn. By extrapolation from high-temperature solubilities, we have assumed that the solubility of Sn is between 1% and 5%. As we mentioned before, we restricted the temperatures to values no higher than the melting-point temperature of the solute. If we relax this restriction, then a few deviations appear in Fig. 3 (also in Fig. 1). Sb and Ga become filled circles. Although the number of exceptions is in both cases

very small, we think that the trends in solid solubility are better displayed by imposing the above-mentioned temperature restriction. In Fig. 4, in which the host metal is Co, a line has also been drawn separating the soluble from the insoluble elements. The only exceptions are Sb, Li, and Ca, but as we stated above, we do not trust the experimental information on these three alloys (the data on Sb are also due to the same author²²). The improvement in the separation of soluble and insoluble elements which Figs. 3 and 4 show with respect to Figs. 1 and 2 can be ascribed to the introduction of the atomic-size coordinate. It also happens that one can approximately draw contours corresponding to increasing degrees of solubility more accurately than in Figs. 1 and 2. To show this we have drawn the broken lines of Figs. 3 and 4. These broken lines are contours containing the elements with high solid solubility (higher than 15%). Only one exception is found (Zn, in Fig. 4). Figures 3 and 4 show that the main factor determining insolubility is the size difference. Alloys with high ΔR_{ws} show solid insolubility, independently of the sign and the size of ΔH_c .²⁴ More work is needed to define precisely the topology of these contours. The two hosts treated in this paper are rather peculiar, because both have a small Wigner-Seitz radius. Hosts with an

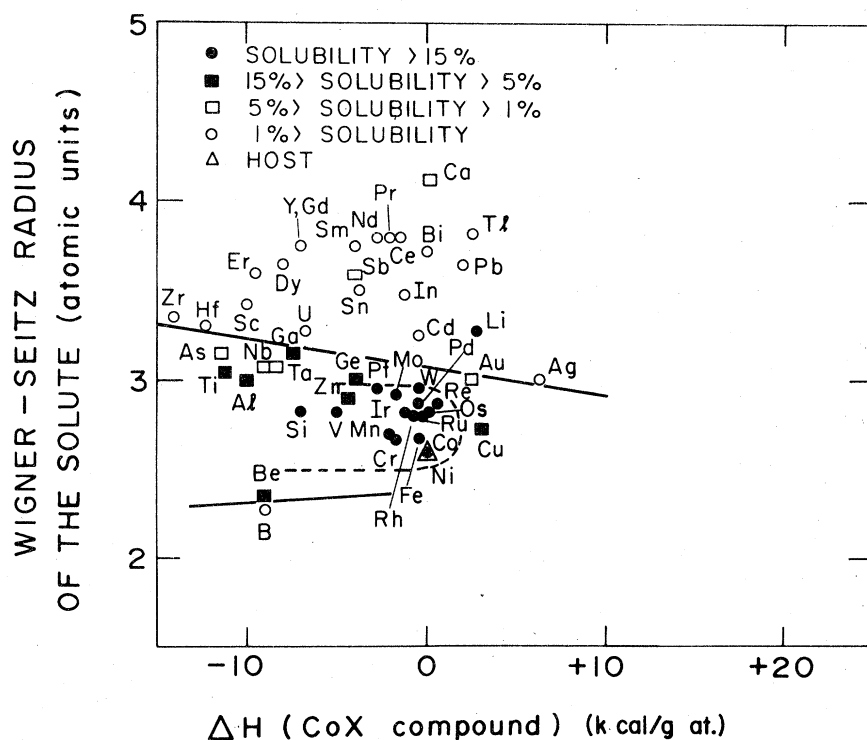


FIG. 4. Same as Fig. 3, although the host is Co. See text for comments on the exceptions.

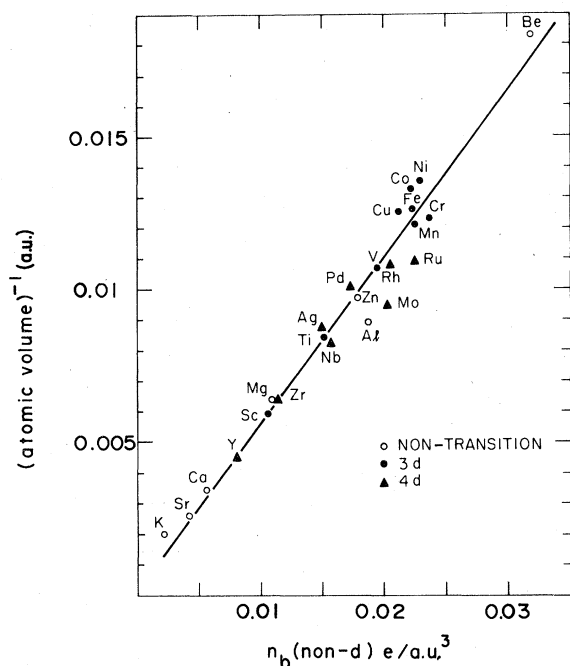


FIG. 5. Inverse of the atomic volume versus the non- d part of the electron density at the boundary of bulk atomic cells.

intermediate volume will help in this task. That work is now in progress. It appears from Figs. 3 and 4 that the line separating the insoluble from the soluble elements (the upper line at least, because it is the only one for which there is enough

information) is not parallel to the ΔH_c axis, but has a nonzero slope. This means, as is well known, that the size difference is not the only factor determining the precise boundary between soluble and insoluble elements. The graphs show that for solutes near the insolubility boundary the size-difference requirement becomes more relaxed as ΔH_c changes from positive to negative values. This is understandable since the size difference ΔV contributes to the heat of solution with a positive energy²⁵:

$$\Delta H_{\text{size}} \propto (\Delta V)^2. \quad (2)$$

The rationalization of the results of Figs. 3 and 4 can be obtained by writing the heat of solution as a sum of three terms:

$$\Delta H_{\text{sol}} = [-P(\Delta\phi^*)^2 - R] + Q(\Delta n_b^{1/3})^2 + M(\Delta V)^2. \quad (3)$$

In order to have a non-negligible solid solubility, ΔH_{sol} should not be too positive; this allows the entropy term $-T\Delta S_{\text{mix}}$ to make the free energy ($\Delta H_{\text{sol}} - T\Delta S_{\text{mix}}$) negative. If ΔV is too big, then the third term in Eq. (3) is the leading one and it makes the solute insoluble, irrespective of the values of $\Delta\phi^*$ and $\Delta n_b^{1/3}$. If ΔV is relatively small, then all three terms in Eq. (3) are important. Then ΔH_{sol} will not be too positive only if the sum of the first two terms is not too positive. This explains why, for a given ΔR_{WS} , solutes with a highly positive ΔH_c show lower solubilities than the other elements.

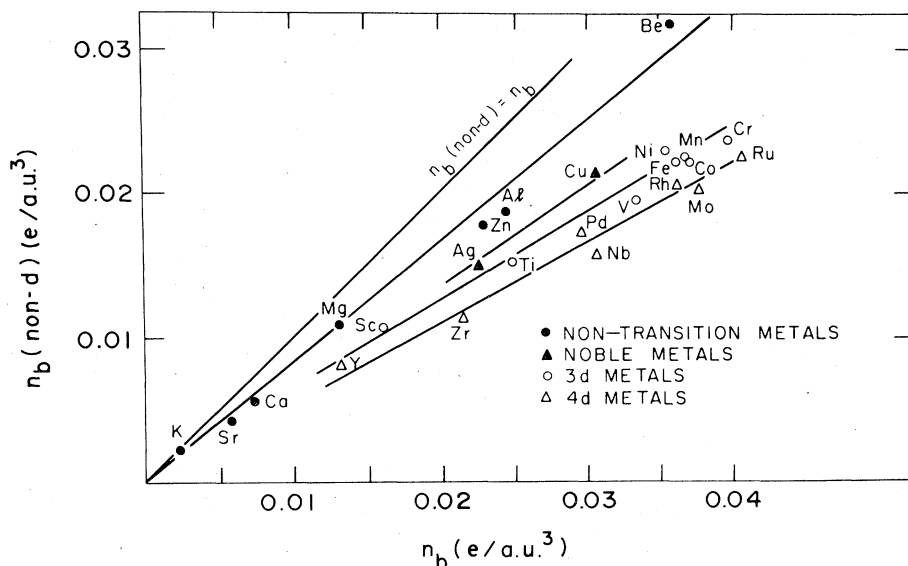


FIG. 6. Non- d part of the electron cell-boundary density versus total cell-boundary density. The line $n_b(\text{non-}d) = n_b$ is included for comparison.

III. COMMENTS

Figures 3 and 4 show that the three-parameter scheme proposed in this paper is more successful than previous two-parameter schemes for predictions of solid solubility in alloys, while at the same time it is very simple to use. As mentioned above, both the Darken-Gurry and Chelikowsky schemes give good first approximations to the problem. This is because atomic size and electron cell-boundary density show a strong correlation. We analyze this correlation in detail in Figs. 5 and 6. Figure 5 is a plot of the inverse of the atomic volume ($V = \frac{4}{3}\pi R_{\text{WS}}^3$) versus the non- d part of the electron cell-boundary density. The non- d part of n_b was calculated by Moruzzi and Williams²⁶ by using the self-consistent augmented spherical wave method.²⁷ A good universal linear relation is found between V^{-1} and n_b (non- d), followed by both transition and nontransition metals. The fact that in nontransition metals n_b (non- d) is rather close to the total n_b shows the equivalence between the use of n_b or V for simple metals. Figure 6 shows n_b (non- d) versus n_b .²⁶ It is found

that a linear relation exists within each class of metals (nontransition metals, noble metals, $3d$ metals, $4d$ metals), but the slope of the line is different in the four different classes of metals. In other words, combining the results of Figs. 5 and 6, we conclude that n_b and V are equivalent parameters within a given class of metals, but only within a given class.

Stronger correlations exist for particular classes of metals. In fact, the solid solubility of nontransition homovalent alloys can be simply explained in terms of a unique parameter for each metal.^{28,29} This is true because, for simple metals with a common valence, ϕ^* , n_b , and V are equivalent parameters.

ACKNOWLEDGMENTS

We thank V. L. Moruzzi and A. R. Williams for providing us with the calculated values of n_b and n_b (non- d). We also acknowledge helpful comments from L. A. Girifalco. One of us (J. A. A.) is grateful to Westinghouse Corporation for financial support.

*Address after September 1, 1980: Departamento de Física Teórica, Universidad de Valladolid, Valladolid, Spain.

¹W. Hume-Rothery, R. E. Smallman, and C. W. Haworth, *Structure of Metals and Alloys*, 5th ed. (Institute of Metals, London, 1969).

²J. Friedel, *Adv. Phys.* **3**, 446 (1954).

³J. D. Eshelby, in *Solid State Physics*, edited by F. Seitz and D. Turnbull (Academic, New York, 1956), Vol. 3, p. 79.

⁴L. S. Darken and R. W. Gurry, *Physical Chemistry of Metals* (McGraw-Hill, New York, 1953).

⁵L. Pauling, *The Nature of the Chemical Bond* (Cornell University Press, Ithaca, 1960).

⁶J. T. Waber, K. Gschneidner, Jr., A. C. Larson, and M. Y. Prince, *Trans. Metall. Soc. AIME* **227**, 717 (1963).

⁷A detailed review of the use of the Darken-Gurry method has been given by K. A. Gschneidner, Jr., *Theory of Alloy Phase Formation*, edited by L. H. Bennett (The Metallurgical Society of AIME, New York, 1980), p. 1.

⁸J. R. Chelikowsky, *Phys. Rev. B* **19**, 686 (1979).

⁹A. R. Miedema, F. R. de Boer, and P. F. de Chatel, *J. Phys. F* **3**, 1558 (1973).

¹⁰A. R. Miedema, *Philips Tech. Rev.* **36**, 217 (1976).

¹¹A. R. Miedema, F. R. de Boer, and R. Boom, *CALPHAD* **1**, 341 (1977).

¹²P. F. de Chatel and G. G. Robinson, *J. Phys. F* **6**, L173 (1976).

¹³J. R. Chelikowsky and J. C. Phillips, *Phys. Rev. B* **17**, 2453 (1978).

¹⁴J. A. Alonso and L. A. Girifalco, *Phys. Rev. B* **19**,

3889 (1979). J. A. Alonso, D. J. González, and M. P. Híquez, *Solid State Commun.* **31**, 9 (1979); J. A. Alonso and L. A. Girifalco, *J. Phys. F* **8**, 2455 (1978).

¹⁵C. H. Hodges, *J. Phys. F* **7**, L247 (1977); *Philos. Mag.* **38**, 205 (1978).

¹⁶D. G. Pettifor, *Phys. Rev. Lett.* **42**, 846 (1979).

¹⁷C. M. Varma, *Solid State Commun.* **31**, 295 (1979).

¹⁸A. R. Williams, C. D. Gelatt, and V. L. Moruzzi, *Phys. Rev. Lett.* **44**, 429 (1980).

¹⁹This point has also been recently stated by A. R. Miedema and P. F. de Chatel, *Theory of Alloy Phase Formation*, edited by L. H. Bennett (The Metallurgical Society of AIME, New York, 1980), p. 344.

²⁰M. Hansen, *Constitution of Binary Alloys* (McGraw-Hill, New York, 1958); R. P. Elliot, *Constitution of Binary Alloys*, first suppl. (McGraw-Hill, New York, 1965); F. A. Shunk, *Constitution of Binary Alloys*, second suppl. (McGraw-Hill, New York, 1969).

²¹W. G. Moffat, *The Handbook of Binary Phase Diagrams* (General Electric, Schenectady, New York, 1978), Vols. 1, 2, and 3.

²²U. Haschimoto, *Nippon Kinzoku Gakkai-Shi* **1**, 177 (1937).

²³A. R. Miedema, *J. Less-Common Met.* **46**, 67 (1976).

²⁴The sign of ΔH_c for FeCe, FeNd, and FeSm is likely to be incorrect, as evidenced by the fact that ordered compounds exist in the phase diagram of these three alloys. The reason is that the parameters ϕ^* and n_b for Ce, Nd, and Sm, not given in Miedema's tables, have been calculated in a rough way by interpolation between La, Y, and Sc. Also, the alloying behavior of the rare earths is rather peculiar and a small modification of the Miedema theory could be needed. For

recent work on some of the rare earths see F. R. de Boer, W. H. Dijkman, W. C. M. Mattens, and A. R. Miedema, *J. Less-Common Met.* 64, 241 (1979). Despite the sign error, Ce, Nd, and Sm are still in the correct region in Fig. 3. The high value of ΔR_{WS} makes this error irrelevant.

²⁵A. R. Miedema, P. F. de Chatel, and F. R. de Boer, *Physica (Utrecht)* 100B, 1 (1980).

²⁶V. L. Moruzzi and A. R. Williams (private communication).

²⁷A. R. Williams, J. Kübler, and C. D. Gelatt, *Phys. Rev. B* 19, 6094 (1979).

²⁸L. A. Girifalco, *Acta Metall.* 24, 759 (1976).

²⁹J. A. Alonso and M. P. Iñiguez, *Physica (Utrecht)*, in press.